nature portfolio

Peer Review File

Spectrally sharp magnetic excitations above the critical temperature in a frustrated Weyl semimetal

Corresponding Author: Mr Michael Terilli

This file contains all reviewer reports in order by version, followed by all author rebuttals in order by version.

Version 0:

Reviewer comments:

Reviewer #1

(Remarks to the Author)
The manuscript presents results of resonant elastic (REXS) and inelastic (RIXS) x-ray scattering experiments on a single crystalline thin film of Y2Ir2O7. The magnon dispersion extracted from RIXS is compared to theoretical dispersion calculated using linear spin wave theory. A broad magnetic continuum observed in RIXS spectra is interpreted based on LDA+U band structure calculations.

Temperature dependent REXS measurements on a structurally forbidden Bragg peak allowed to confirm q=0 magnetic order in Y2Ir2O7. The dispersion of the magnetic excitations was measured using RIXS at 10 K. After subtracting an elastic peak and magnetic continuum Authors observed two gapped magnetic excitation. Measuring RIXS spectra at the Ir LIII edge on a thin film of Y2Ir2O7 is a challenging task and I greatly appreciate the results. However, similar RIXS measurements have already being performed before on single crystals of Sm2Ir2O7 [46] and Eu2Ir2O7 [51] and gapped magnetic excitations were observed in both compounds. To my opinion, the results presented in the manuscript do not contain new physics and are more appropriate for a specialized journal.

What is new, and seems to be the main selling point of the paper, is the observed persistence of gapped magnetic excitations at the Gamma point even above T_N which Authors relate to cooperative paramagnetism. However, this interesting and important observation contradicts to the results of RIXS measurements on Eu2Ir2O7 published in Ref. [51] in which softening of the magnetic mode at Gamma is observed as temperature approaches T_N. On the other hand, the excitation at a zone boundary survives even above T_N which suggests that symmetry lowering caused by magnetic order disappears above T_n. A possible source of this discrepancy should be discussed in the manuscript.

Another discrepancy to the previously published RIXS spectra is the observation of two magnetic excitations while only one magnon was detected in Refs. 46 and 51 although the experiments where done on bulk single crystals. What is the reason for this discrepancy? Is the resolution of the RIXS set up used by Authors so much better?

I am also confused by the use of non-spin-polarized LDA+U band structure calculations, called paramagnetic in the manuscript, for interpretation of the RIXS data. According to the RIXS data presented in the manuscript and in Ref. 51 Ir local moments exist also above T_N but are disordered. In order to

model such a paramagnetic state one needs to use either dynamical mean-filed (DMFT) or the so-called disorder local moments (DLM) approach. Instead Authors seem to simply perform LDA+U calculations neglecting spin polarization of Ir d states. In this case Ir jeff=1/2 bands remain half-filled (n_i~1/2) and, thus, almost unaffected by the orbital dependent LDA+U potential which can be crudely approximated as V_i=(U-J)(1/2-n_i) where n_i is the orbital occupation. The only effect of U in this case is to shift fully occupied Ir jeff=3/2 bands to lower energy. I do not see any physical reason why these non-spin-polarized calculations can describe excitations in a paramagnetic state with disordered Ir local moments. (It would be helpful to specify in the details section which implementation of the LDA+U method was used.)

According to published resistivity data Y2Ir2O7 shows non-metallic behavior at low temperatures. Why so much attention is paid in the manuscript to Weyl points which may appear in LDA+U calculations for all-in-all-out order if a sufficiently small value of U is used?

In view of the above mentioned comments I cannot recommend to publish the manuscript in its present form.

(Remarks on code availability)

Reviewer #2

(Remarks to the Author)
The paper investigates the magnetic properties of thin films of the pyrochlore iridate compound Y2Ir2O7, a material that has attracted significant attention in recent years due to its unique combination of properties highly relevant to quantum condensed matter. These include strong electronic correlations, geometric frustration, large spin-orbit coupling, and topological electronic band structures. As a result, experimental studies on this material class are of considerable interest to a broad scientific audience. The paper focuses on the spectrum of magnetic excitations, employing resonant elastic and inelastic X-ray scattering. This is a particularly valuable approach given the challenges associated with other scattering techniques, such as neutron scattering, which are hindered by iridium's high absorption cross-section. The authors present experimental evidence of sharp, gapped magnetic excitations that persist well above the Néel temperature, suggesting the presence of an extended cooperative paramagnetic phase. This phase lies between the low-temperature ordered phase and the conventional high-temperature paramagnetic state, potentially representing the first experimental realization of the theoretically predicted "quasi-universal" regime near the quantum critical point in pyrochlore iridates. The experimental findings are compared to spin-wave analysis using an effective spin-1/2 model, and further supported by dynamical susceptibility calculations based on ab initio density functional theory.

In my view, this paper holds significant potential. However, in its current form, several statements appear unclear or insufficiently supported by the presented data.

(1) The abstract mentions that the sharp magnetic excitations suggest "the existence of a hidden degree of freedom coupling to the magnetic fluctuations." In my opinion, this statement is not sufficiently elaborated on in the interpretation part of the manuscript. What kind of hidden degree of freedom do the authors have in mind? What is the evidence for this hidden degree of freedom?

(2) Fig. 1b: The figure suggests that the cooperative paramagnetic phase for Y2Ir2O7 remains until 190 K, which is the temperature where the onset of hysteretic behavior in powder samples has been observed in Ref. 48. Usually, one would expect the system to transition from the cooperative paramagnet to the usual paramagnet via a smooth crossover, but, of course, an (unnecessary) first-order phase transition is not excluded. I do not find it obvious why the transition scale between the cooperative paramagnet and the usual paramagnet in the single crystals should coincide with the onset temperature of hysteretic behavior observed in the powder samples. Can the authors explain this? Furthermore, do the authors also observe features of a sharp transition at 190 K in their single crystals? As a minor point, the abbreviation "XRMS" used in the label should be defined.

(3) The fit of the scattering intensity versus the reduced temperature should be shown explicitly. It is not obvious that the data yields the exponent $\beta = 0.33$, indicative of the 3D Ising universality class. As different universality classes are often distinguished by only small deviations in the values of critical exponents, it is also necessary for the reader to know how stable the fit with respect to different values of β is.

(4) Is the magnetic continuum, which is subtracted from the inelastic scattering signal, temperature independent? From what I understand from Sec. S4 in the Supplementary Information, this seems to be the case; however, I feel this is an important information that should be mentioned explicitly in the main text.

(5) In the context of the interpretation of the magnetic continuum, the authors mention "the spontaneous decay of the magnon modes" as a possible origin. What kind of magnon decay do the authors have in mind? (Scattering of magnons with

electronic degrees of freedom? Multi-magnon decay? Something else?)

(6) It is interesting that the observed sharp magnon dispersion is very flat; namely, the band width appears to be significantly smaller than the gap, and the two bands appear to be well separated. This is a remarkable feature, which is also not well reproduced by the spin-wave calculation and the ab-initio dynamical susceptibility calculations. Do the authors understand the origin of this phenomenon?

(7) In the spin-wave analysis, a model with Heisenberg, Dzyaloshinskii–Moriya, and symmetric off-diagonal Gamma interaction is used. Symmetry would allow, however, a Kitaev-type bond-dependent interaction, see, e.g., [Phys. Rev. X 1, 021002 (2011); Phys. Rev. B 95, 094422 (2017)]. It is not obvious to me why this exchange interaction can be neglected. To the contrary, it would be interesting to know whether taking this interaction into account can improve the agreement between experiment and spin-wave analysis.

(8) What is the evidence for the statement that "the ratio between the competing interactions, D/J ~ 0.17, is in line with the experimental value of T_N = 145 K"? What is the theoretical value of T_N in the model with J = 33.9meV and D = 5.6 meV?

(9) Fig. 4b: The figure shows a metallic density of states, but the caption mentions "the paramagnetic state [...] above the topologically-trivial insulator phase". This should be explained.

(9) Fig. 4c: What is the integration volume around the Brillouin zone center used in this plot? It is confusing that Fig. S6c in the Supplementary Information indicates that the gap of the magnetic excitations at the Brillouin zone center is smaller than a few meV, and possibly zero, while Fig. 4c and the main text, mentioning a "low-energy peak centered around 25 meV", implicitly suggest a finite gap. This should be explained.

(10) The statement that "the signs of the zero-temperature transition from the PyIr Weyl semimetal to the paramagnetic metallic phase are attributed to [...] the emergence of gapless fermions due to the breaking of an emergent internal SO(3) symmetry (Ref. 27)" is confusing. First, at the quantum critical point discussed in Ref. 27, additional gapless fermions are not expected to emerge, since both sides of the transition are semimetallic. Second, it is not clear what is meant with breaking of an emergent symmetry. In my understanding, a symmetry cannot be both emergent and broken at a single point in parameter space.

In conclusion, the paper presents significant experimental results that could be of great interest to a broad audience. However, the current version lacks clarity in the interpretation of the data. I recommend inviting the authors to submit a substantial revision of the manuscript.

(Remarks on code availability)

Version 1:

Reviewer comments:

Reviewer #1

(Remarks to the Author)
Authors answered all my questions and made appropriate changes to the manuscript. The paer can be published in its present form.

(Remarks on code availability)

Reviewer #2

(Remarks to the Author)
In response to the first round of reports, the authors have substantially revised their manuscript. The revision, together with the detailed response, satisfactorily addresses all questions and criticism raised. I recommend to publish the revised manuscript in Nature Communications.

(Remarks on code availability)

Open Access This Peer Review File is licensed under a Creative Commons Attribution 4.0 International License, which permits use, sharing, adaptation, distribution and reproduction in any medium or format, as long as you give appropriate credit to the original author(s) and the source, provide a link to the Creative Commons license, and indicate if changes were made.
In cases where reviewers are anonymous, credit should be given to 'Anonymous Referee' and the source.
The images or other third party material in this Peer Review File are included in the article's Creative Commons license, unless indicated otherwise in a credit line to the material. If material is not included in the article's Creative Commons license and your intended use is not permitted by statutory regulation or exceeds the permitted use, you will need to obtain permission directly from the copyright holder.
To view a copy of this license, visit https://creativecommons.org/licenses/by/4.0/

REVIEWER COMMENTS

Reviewer #1 (Remarks to the Author):

The manuscript presents results of resonant elastic (REXS) and inelastic(RIXS) x-ray scattering experiments on a single crystalline thin film of Y2Ir2O7. The magnon dispersion extracted from RIXS is compared to theoretical dispersion calculated using linear spin wave theory. A broad magnetic continuum observed in RIXS spectra is interpreted based on LDA+U band structure calculations.

(Temperature dependent REXS measurements on a structurally forbidden Bragg peak allowed to confirm q=0 magnetic order in Y2Ir2O7. The dispersion of the magnetic excitations was measured using RIXS at 10 K. After subtracting an elastic peak and magnetic continuum Authors observed two gapped magnetic excitation. Measuring RIXS spectra at the Ir LIII edge on a thin film of Y2Ir2O7 is a challenging task and I greatly appreciate the results. However, similar RIXS measurements have already being performed before on single crystals of Sm2Ir2O7 [46] and Eu2Ir2O7 [51] and gapped magnetic excitations were observed in both compounds. To my opinion, the results presented in the manuscript do not contain new physics and are more appropriate for a specialized journal.

We thank the referee for these comments. Here, we emphasize that the observation of dispersive modes linked to the 4i-4o (4-in-4-out or all-in-all-out) ground state in $Y_2Ir_2O_7$ is itself an important result.

As illustrated by the phase diagram in Fig. 1 of the main text, significant changes take place across the phase diagram with the decrease of rare earth ionic radius. Notably, the Y-based compound is located far away from the Eu and Sm compounds and experiences more local trigonal distortions due to the significantly smaller ionic radius (Y^{3+} 101.9 pm vs. Eu^{3+} 106.6 pm and Sm^{3+} 107.9 pm). Such distortions perturb the delicate balance among crystal-field effects, exchange interactions, and electronic bandwidth and can strongly affect the $J_{1/2}$ and $J_{3/2}$ spin-orbital states. For instance, a sufficiently large crystal-field splitting can preserve a predominantly $J_{1/2}$-based electronic and spin structure with minimal $J_{3/2}$ mixing. As direct evidence, our RIXS data in Fig. R1 show that the relative intensities of the $J_{1/2}$→$J_{3/2}$ transitions differ markedly between $Eu_2Ir_2O_7$ and $Y_2Ir_2O_7$, indicating distinct local environments.

This difference likely contributes to the higher-energy magnon mode deviation from linear spin-wave theory at Γ (Fig. S7 of the Supplementary Material). which implies that higher-order interactions (e.g., ring exchange) may be necessary [Coldea et al., Phys. Rev. Lett. 86, 5377 (2001)]. Due to the geometrical limitations from the thin-film nature of the sample, at this stage, we were not able to resolve the complete magnon dispersion along all high symmetry directions. The improvement in the synthesis of high-quality bulk single crystals may clarify the role of higher-order exchange corrections and yield a more complete picture of spin-wave dynamics in $Y_2Ir_2O_7$.

Alternatively, the random-phase approximation (RPA) framework with intermediate U (rather than the strong electron correlation strength assumed by spin-wave theory) may be more appropriate for some pyrochlore iridate compounds [Lee et al., Phys. Rev. B 87, 214416 (2013)]. In corroboration with our results, recent work on non-stoichiometric $Tb_2Ir_2O_7$ also signals that the RPA approach may better fit the dispersion of the smaller rare-earth site pyrochlore iridate compounds [Faure, Q. et al. ArXiv:2404.03829 (2024).]

We have added the following to the discussion of the low-temperature RIXS results:

"We note that the linear spin-wave fit does not fully capture the behavior of the higher-energy mode near Γ. One possibility is that higher-order interactions (e.g., ring exchange) may be necessary to fully capture the spin-wave behavior [Coldea et al., Phys. Rev. Lett. 86, 5377 (2001)]. The improvement in the synthesis of high-quality bulk single crystals may allow for the study of dispersion along more high-symmetry directions, clarifying the role of higher-order corrections in the spin-wave dynamics in $Y_2Ir_2O_7$. Alternatively, calculating the dynamical structure factor within the random-phase approximation (RPA) may be more appropriate for some pyrochlore iridate compounds [Lee et al., Phys. Rev. B 87, 214416 (2013)]; recent work on non-stoichiometric $Tb_2Ir_2O_7$ also signals that the RPA approach may better fit the dispersion of the smaller rare-earth site pyrochlore iridate compounds [Faure, Q. et al. ArXiv:2404.03829 (2024)]."

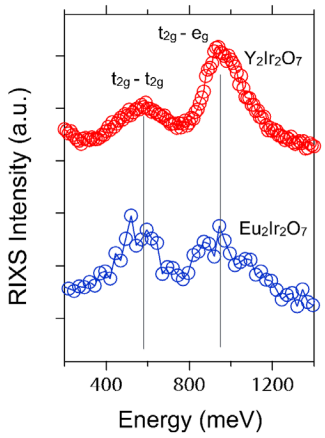

Figure R1: RIXS data for $Y_2Ir_2O_7$ and $Eu_2Ir_2O_7$. The two peaks at ~600 meV and ~1000 meV correspond to t_{2g} -> t_{2g} and t_{2g} -> e_g transitions, respectively. The ratio of the intensity of these peaks differs between these two compounds [unpublished].

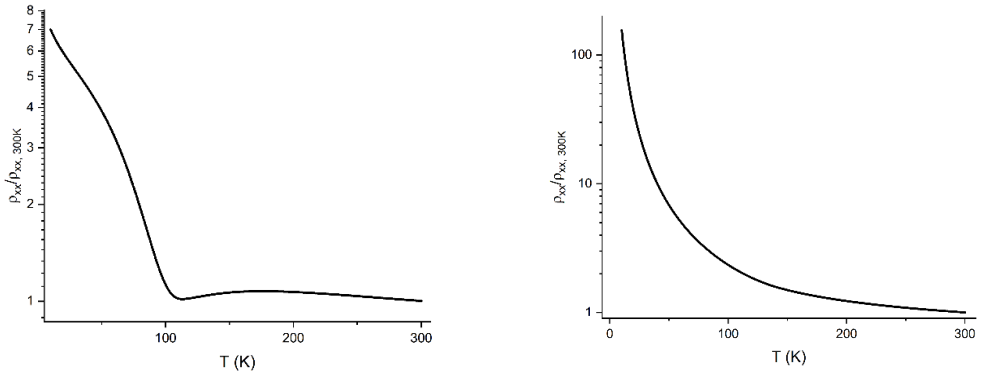

Figure R2: Temperature-dependent resistivity curves for (left) $Eu_2Ir_2O_7$ and (right) $Y_2Ir_2O_7$.

What is new, and seems to be the main selling point of the paper, is the observed persistence of gapped magnetic excitations at the Gamma point even above T_N which Authors relate to cooperative paramagnetism. However, this interesting and important observation contradicts to the results of RIXS measurements on Eu2Ir2O7 published in Ref. [51] in which softening of the magnetic mode at Gamma is observed as temperature approaches T_N. On the other hand, the excitation at a zone boundary survives even above T_N which suggests that symmetry lowering caused by magnetic order disappears above T_n. A possible source of this discrepancy should be discussed in the manuscript.

We thank the referee for recognizing the main result of our paper, namely the persistence of the magnetic excitations above T_N. As discussed above, the iridates containing Eu and Y ions are far apart on the phase diagram (Figure 1b, main text). A comparison between our $Y_2Ir_2O_7$ and the $Eu_2Ir_2O_7$ data from Ref. [51] demonstrates several key differences between these systems. First, we note that the critical exponent $\beta = 0.3$ that we found in $Y_2Ir_2O_7$ is in excellent agreement with $\beta \approx 0.33$ predicted for the 3D Ising class [Odor, G., Rev. Mod. Phys. 76, 663 (2004)]. In contrast, Ref. [51] reports a critical exponent $\beta = 0.2$, for $Eu_2Ir_2O_7$ demonstrating a sharper change in the REXS intensity as T approaches T_N and a divergence from the Ising-like (discrete magnetic Hamiltonian) symmetry case.

Concerning the precise cause of this difference, here we conjecture a few possibilities:

One possibility is that such a contrast arises from differences in the rare-earth ionic radius. Due to the large spin-orbit coupling of ~ 0.5 eV the $J_{1/2}$ manifold wavefunction entangles Ir 5d spin and orbital degrees of freedom. Thus, with the change in rare-earth radius, the Ir-O-Ir bond length and bond angle change across the R series, leading to a deviation of the $J_{1/2}$ significantly away from the idealized equal superposition of d_{xy}, d_{yz}, d_{zx} Ir orbitals [G. Jackeli and G. Khaliullin, Phys. Rev. Lett. 102, 017205 (2009)]. Across the Néel transition, as there is no structural phase transition, the unchanged lattice coupling may lead to a persistent magnetic excitation in $Y_2Ir_2O_7$.

We also note that $Eu_2Ir_2O_7$ undergoes a metal-insulator transition at T_N (Figure R2a) with an unexpectedly large renormalization of the AFM exchange parameter J, to the extent that the authors of [51] conclude that "Thus, our observation strongly suggests that $Eu_2Ir_2O_7$ cannot be described with a local moment model satisfactorily." In our case, we can explain the magnetic properties of $Y_2Ir_2O_7$ satisfactorily within a local moment model.

We further compare the transport properties of $Y_2Ir_2O_7$ and $Eu_2Ir_2O_7$, which also differ markedly (see Figure R2). The $Eu_2Ir_2O_7$ film exhibits a clear minimum at T_N = 105 K, characteristic of a metal-to-insulator transition. In contrast, $Y_2Ir_2O_7$ does not display any apparent signature of such a transition and instead shows a small-gap semiconducting behavior [Liu, X. et al. Appl. Phys. Lett. 117, 041903 (2020)]. $Y_2Ir_2O_7$ seems to be a more likely candidate for observing $T > T_N$ magnetic excitations since there is no confounding transition (e.g., structural) in other degrees of freedom at the same critical temperature (as seen in Figure R2b). Since there is no structural phase transition across the Néel transition

in $Y_2Ir_2O_7$, the persistent strength of spin-lattice coupling could support the spectrum of persistent magnetic excitations.

Finally, based on the previous torque measurements on $Eu_2Ir_2O_7$ [Liang, T. et al. Nat. Phys. 13, 599-603 (2017)] one can conjecture that that the observed paramagnon modes could be connected to the hidden magnetic order that develops at room temperature and coexists with the 4i-4o phase below T_N.

We have added the following to the discussion of the phase diagram:

"The rare-earth element has a significant impact on the structural and electronic properties of the pyrochlore iridates. Like the other compounds on the left-hand side of the diagram, $Y_2Ir_2O_7$ exhibits semiconducting behavior (see Supplementary Information Fig. S2), sharply contrasting with the metallic behavior for R=Eu and beyond."

We add the following line to the REXS discussion:

"We note that this value differs from the critical exponent β=0.2 as found in $Eu_2Ir_2O_7$ (hereafter $Eu_2Ir_2O_7$) [Chun, S. H. et al., Phys. Rev. Lett. 120, 177203 (2018)]. This finding, in conjunction with the difference in resistivity behavior near T_N, implies that the magnetic behavior in $Y_2Ir_2O_7$ may be markedly different compared to $Eu_2Ir_2O_7$."

We also expand upon the following sentences on the discrepancy between our results and those in [51]:

"The persistence of the unusual magnetic gap, even as the long-range magnetic order melts, is unexpected and unique, standing in sharp contrast to the previous RIXS reports on pyrochlore iridates. $Sm_2Ir_2O_7$ shows the spectral weight for the magnon mode disappear around the transition temperature [Donnerer, C. et al., Phys. Rev. Lett. 117, 037201 (2016)], whereas $Eu_2Ir_2O_7$ shows the gap softening at Γ as T approaches T_N [Chun, S. H. et al., Phys. Rev. Lett. 120, 177203 (2018)]. $Y_2Ir_2O_7$ is perhaps a more likely candidate for observing the persistent gapped magnetic excitations since the system lacks a confounding structural phase transition or the renormalization of the Heisenberg interaction observed in $Eu_2Ir_2O_7$. We speculate that this could result from Ir-O-Ir bond angle and Ir-O bond length differences across the pyrochlore iridate family, leading to a deviation of the $J_{1/2}$ significantly away from the idealized equal superposition of Ir d_{xy}, d_{yx} and d_{zx} orbitals [G. Jackeli and G. Khaliullin, Phys. Rev. Lett. 102, 017205 (2009)]."

We have also added Figure R2 and its caption to the Supplementary Information, along with the following description:

"To compare the resistivity behavior between $Y_2Ir_2O_7$ and $Eu_2Ir_2O_7$, electrical transport measurements were taken between 2K and 300K. Measurements were taken at Rutgers University with a Physical Properties Measurement System manufactured by Quantum

Design. Fig. S2 shows that $Eu_2Ir_2O_7$ has a minimum in resistivity around 105 K, indicating a metal-insulator transition at T_N. $Y_2Ir_2O_7$ lacks such a transition, instead resembling more semimetallic behavior."

Another discrepancy to the previously published RIXS spectra is the observation of two magnetic excitations while only one magnon was detected in Refs. 46 and 51 although the experiments where done on bulk single crystals. What is the reason for this discrepancy? Is the resolution of the RIXS set up used by Authors so much better?

We thank the referee for the insightful comment. We believe the RIXS resolution of our setup is comparable to that reported in Refs. [46] and [51]. Theoretically, based on the spin-wave analysis, there are four branches of magnetic excitations (as detailed in Supplementary Information S7). Given the current RIXS resolution of 28 meV and considering that at least two of the four branches are closely spaced in energy at the same value of momentum q, it is experimentally possible to resolve 2–3 branches under most optimal conditions.

To ensure a conservative yet robust analysis, we have modeled the system using two magnon branches. This choice represents the maximum number required to stabilize the fit while maintaining a good agreement with our RIXS data and avoiding overparameterization of the fitting routine.

The main distinction between our work and previous studies lies in the grazing-angle scattering geometry used in the experiment. This geometry is necessitated by the high penetration depth of the X-ray and the smaller diffraction volume available in $Y_2Ir_2O_7$ thin films. It is well known that the RIXS cross-section for different excitation branches is strongly dependent on the scattering geometry and similar effect can be at play here [J. Kim et al., Nat. Commun. 5, 4453 (2014)]. To resolve this problem, a thorough study would be desired e.g., in bulk high-quality single crystals (not available yet), but not in thin films with severe geometrical constraints.

Additionally, the experimental magnitude of the magnon spectral weight is influenced by the specific nature of the magnetic excitations. In our measurements, the magnetic spectral weight is significantly stronger than that observed in Sr_2IrO_4 films of similar thickness. Specifically, the magnon peak in our data is approximately 30% of the elastic line intensity, compared to around 10% in the Sr_2IrO_4 films. This difference can be attributed in part to the higher quality of our films and in part to the intrinsic differences between the two materials (pyrochlore $Y_2Ir_2O_7$ vs. layered perovskite Sr_2IrO_4). To comprehensively understand these effects, as we suggested earlier in the last paragraph, a systematic study of the incident-angle dependence of the RIXS spectra for bulk quality crystalline pyrochlore iridates would be desirable.

I am also confused by the use of non-spin-polarized LDA+U band structure calculations, called paramagnetic in the manuscript, for interpretation of the RIXS data. According to the RIXS data presented in the manuscript and in Ref. 51 Ir local moments exist also above T_N but are disordered. In order to model such a paramagnetic state one needs to use either dynamical mean-filed (DMFT) or the so-called disorder local moments (DLM) approach. Instead Authors seem to simply perform LDA+U calculations neglecting spin polarization of Ir d states. In this case Ir jeff=1/2 bands remain half-filled (n_i~1/2) and, thus, almost unaffected by the orbital dependent LDA+U potential which can be crudely approximated as V_i=(U-J)(1/2-n_i) where n_i is the orbital occupation. The only effect of U in this case is to shift fully occupied Ir jeff=3/2 bands to lower energy. I do not see any physical reason why these non-spin-polarized calculations can describe excitations in a paramagnetic state with disordered Ir local moments. (It would be helpful to specify in the details section which implementation of the LDA+U method was used.)

We thank the referee for raising the point regarding our calculations of the paramagnetic phase. To address this, we have now performed DFT+eDMFT calculations for the paramagnetic phase. The results, including details of the density of states (DOS) and spectral function obtained using DMFT, are presented in Figure R3, along with a comparison with DFT+U results.

For the paramagnetic phase, the metal-insulator-transition happens around U=5.0 eV (see below for explanations of the value of U). The quasiparticle peak of the J_{eff}=½ band is highly suppressed at U=4.5 eV and disappears at U=5.0 eV. The calculations of the spin susceptibility from the eDMFT Green's function are beyond the scope of our work. We note, however, that the eDMFT GDOS of the paramagnetic system for U up to 4.0 eV still shows the two-peak structure, similar to that seen in DFT+U. The main difference is that now the separation of the two peaks is about 200 meV. Therefore, we conclude that the susceptibility from eDMFT is likely to show a similar behavior to that from DFT+U, but with a shifted magnon peak.

Now, we have also clarified the details about the DFT+U calculations in the method part:

""We used the rotationally invariant approach for DFT+U [Dudarev et al., PRB 57, 1505 (1998)], with a single Hubbard U parameter correlating the d-shell of the Ir sites. Comparisons of the electronic structures obtained from DFT+eDMFT are provided in the Supplementary Material sections S12 and S13."

Additionally, we have included a short section in the supplementary material to compare DFT+eDMFT results:

In this section, we present the results of the electronic structure calculations obtained using DFT+embedded dynamical mean-field theory (eDMFT) for the paramagnetic phase of Y2Ir2O7. The DFT part of the calculation is performed using the WIEN2K code [38], using an

all-electron LAPW basis set and a PBE exchange-correlation functional on a Monkhorst-Pack mesh of 11x11x11 k points. We have thoroughly checked that the electronic structures obtained by the VASP and WIEN2K agree when U=0. The eDMFT calculations [39-41] start with projecting to a set of real-space orbitals that span the correlated subspace, and the bath orbitals are treated by DFT. The hybridization between the impurity and the bath is then self-consistently determined by solving the DMFT equations. The projector is chosen to be the atomic-like t2g orbitals of one isolated Ir atom. A window of 20 eV around the Fermi level is used for computing the hybridization between the impurity and the bath, and during the self-consistency loops, continuous time quantum Monte Carlo [42, 43] was performed to solve the quantum impurity until the charge density, the impurity self-energy, and the lattice Green's function are converged. The double-counting correction is computed using the nominal double-counting scheme [39, 43]. Then the maximum entropy method [44] is used to perform the analytical continuation of the self-energy to real frequencies.

Figure S11 shows a comparison between the electronic structures of bulk $Y_2Ir_2O_7$ computed using DFT+eDMFT (a-b, paramagnetic state) and DFT+U (c-d, zero local spin magnetic moments are assumed).
We notice that eDMFT captures the metal-insulator transition of the system around U=5.0 eV. In contrast, when using DFT+U, the system remains metallic even with a large U. This is because in our DFT+U calculations, we have constrained the local spin magnetic moments to be zero. The on-site spin fluctuations would only be accessible if the disordered local moments approach [45] is used. We highlight the similar two-peak feature in the DOS that appears at the Fermi level in the metallic regime from both DFT+U and DMFT results, suggesting that one would expect to see a similar behavior in their transverse spin susceptibilities."

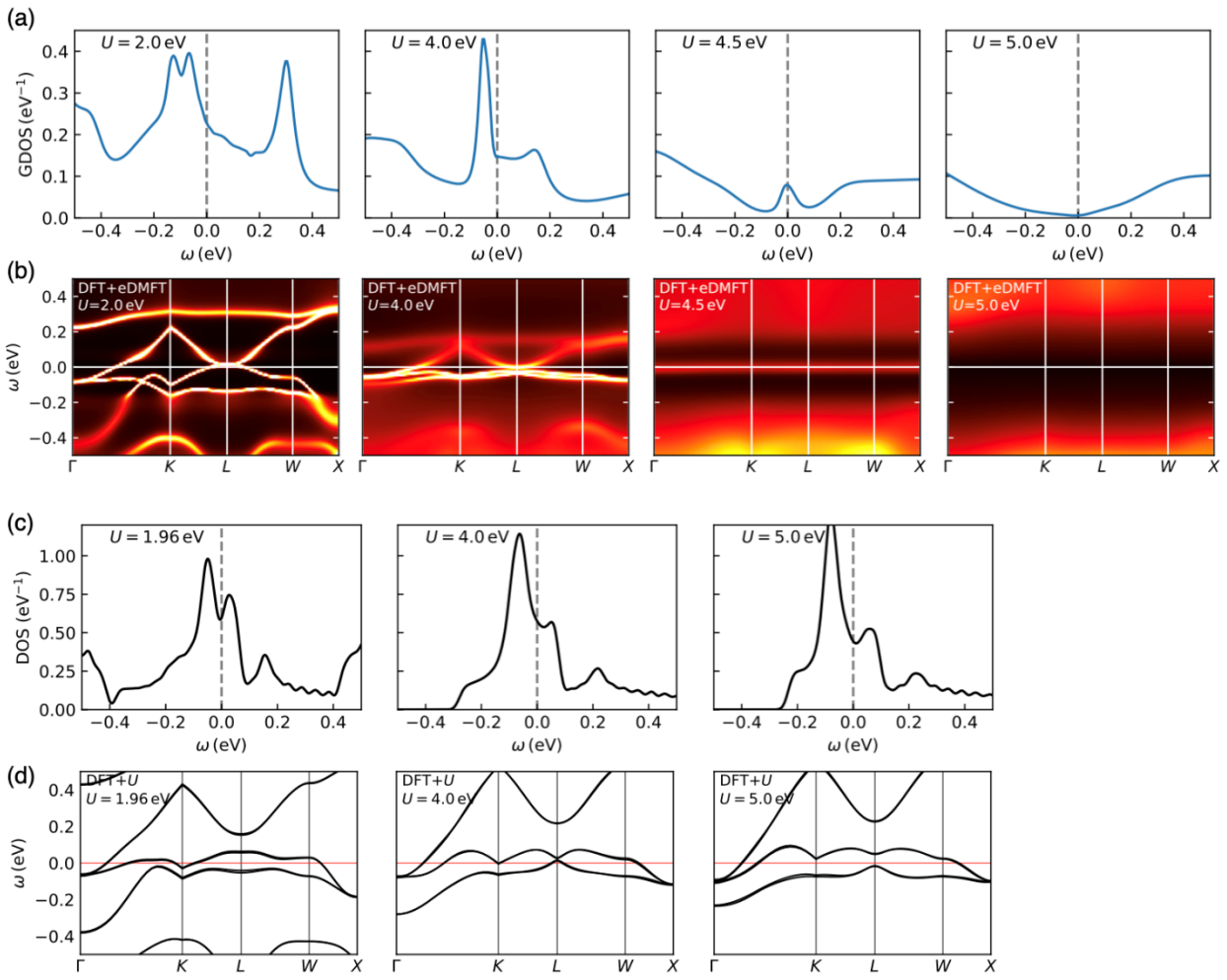

Figure R3: A comparison between the electronic structures of bulk Y2Ir2O7 obtained using DFT+U (zero local spin magnetic moments) and DFT+eDMFT (paramagnetic state)

(a) The global density of states (GDOS) and (b) the spectral functions of the paramagnetic state computed using DFT+eDMFT, with U=2.0,4.0,4.5 eV, J=0.8 eV, and β=50 meV. (c) The density of states (DOS) and (d) the band structures as given by DFT+U, with U=1.96,4.0,5.0 eV. See the details of the DMFT calculations in the text. Note that for DFT+eDMFT, larger U significantly decreases the bandwidth of the J_{eff}=1/2 bands and eventually brings the system from a metallic to an insulating state around 5 eV. This is not captured with our calculations using DFT+*U* where the zero on-site spin magnetic moments are assumed.

According to published resistivity data Y2Ir2O7 shows non-metallic behavior at low temperatures. Why so much attention is paid in the manuscript to Weyl points which may appear in LDA+U calculations for all-in-all-out order if a sufficiently small value of U is used?

We thank the reviewer for raising this question. First, we note that the term 'Weyl semimetal,' along with the associated Weyl points, is used as a label for $Y_2Ir_2O_7$ and the broader class of rare-earth pyrochlore iridates based on observed transport behaviors.

As shown in [X. Liu et al., Nat. Commun. 15:10348 (2024)], thin films of $Y_2Ir_2O_7$ exhibit an anomalous Hall conductivity (σ_{AHE}) for $T < T_N$, consistent with theoretical predictions for a magnetic Weyl semimetal state. Additionally, the resistivity behavior, $\rho(T) \propto T^{-4}$, observed in $Y_2Ir_2O_7$ [LaBarre, P.G. et al., J. Phys.: Condens. Matter 32 (2020)] provides further evidence supporting the presence of the Weyl semimetal phase.

We also appreciate the referee's point regarding the 'LDA+U' calculations. To address this, we have clarified this aspect in the section titled 'Density Functional Theory Calculations' as follows:

"We have identified the range $U \leq 0.9$ eV as the region where the ground state exhibits a Weyl semimetal phase (with small electron and hole pockets near $U = 0.9$ eV), beyond which the system transitions to an insulating state. See Supplementary Information, Section S9, for additional details. As seen, the 4-in/4-out magnetic ordering remains robust for all values of $U \geq 0.75$ eV. We estimated the ground state to appear for $U = 1.96$ eV for the Ir *d*-orbitals using the linear response theory within DFT+U [Cococcioni, M. & de Gironcoli, S. Phys. Rev. B 71, 035105 (2005).], where the ground state of Y2Ir2O7 appears as a 4i-4o insulator with a small gap of 0.38 eV."

All discussion corresponding to sufficiently small U (≤ 0.9 eV), which represent the Weyl semimetal phase, have now been moved to the supplementary information.

Reviewer #2 (Remarks to the Author):

The paper investigates the magnetic properties of thin films of the pyrochlore iridate compound Y2Ir2O7, a material that has attracted significant attention in recent years due to its unique combination of properties highly relevant to quantum condensed matter. These include strong electronic correlations, geometric frustration, large spin-orbit coupling, and topological electronic band structures. As a result, experimental studies on this material class are of considerable interest to a broad scientific audience. The paper focuses on the spectrum of magnetic excitations, employing resonant elastic and inelastic X-ray scattering. This is a particularly valuable approach given the challenges associated with other scattering techniques, such as neutron scattering, which are hindered by iridium's high absorption cross-section. The authors present experimental evidence of sharp, gapped magnetic excitations that persist well above the Néel temperature, suggesting the presence of an extended cooperative paramagnetic phase. This phase lies between the low-temperature ordered phase and the conventional high-temperature paramagnetic state, potentially representing the first experimental realization of the theoretically predicted "quasi-universal" regime near the quantum critical point in pyrochlore iridates. The experimental findings are compared to spin-wave analysis using an effective spin-1/2 model, and further supported by dynamical susceptibility calculations based on ab initio density functional theory.

In my view, this paper holds significant potential. However, in its current form, several statements appear unclear or insufficiently supported by the presented data.

(1) The abstract mentions that the sharp magnetic excitations suggest "the existence of a hidden degree of freedom coupling to the magnetic fluctuations." In my opinion, this statement is not sufficiently elaborated on in the interpretation part of the manuscript. What kind of hidden degree of freedom do the authors have in mind? What is the evidence for this hidden degree of freedom?

We thank the reviewer for this comment. We recognize that the statement in question was not fully aligned with the main message of the manuscript. We now highlight the universal regime as mentioned in the main text: “Furthermore, the identified unconventional CP phase could be the first realization of the exotic 'quasi-universal' regime theoretically predicted to arise in the critical fan above the quantum critical point (QCP) in the PyIr family.”

To reflect this, we have revised the abstract as follows:

“...we unequivocally reveal the presence of spectrally sharp, gapped magnetic excitations in $Y_2Ir_2O_7$ that surprisingly persist well above the Néel transition temperature, signaling the presence of a quasi-universal regime connected to fluctuations on frustrated lattices.”

(2) Fig. 1b: The figure suggests that the cooperative paramagnetic phase for Y2Ir2O7 remains until 190 K, which is the temperature where the onset of hysteretic behavior in powder samples has been observed in Ref. 48. Usually, one would expect the system to transition from the cooperative paramagnet to the usual paramagnet via a smooth crossover, but, of course, an (unnecessary) first-order phase transition is not excluded. I do not find it obvious why the transition scale between the cooperative paramagnet and the usual paramagnet in the single crystals should coincide with the onset temperature of hysteretic behavior observed in the powder samples. Can the authors explain this? Furthermore, do the authors also observe features of a sharp transition at 190 K in their single crystals? As a minor point, the abbreviation "XRMS" used in the label should be defined.

We thank the referee for this comment. We agree that the onset of the cooperative paramagnetic (CP) phase may not necessarily coincide with the onset of hysteretic behavior.

Regarding the question of hysteretic behavior in our thin films: due to the small volume of our film (5 mm × 5 mm × 100 nm thickness) and the substantial contribution from the substrate (5 mm × 5 mm × 1 mm), high-resolution SQUID measurements cannot reliably detect the presence of hysteresis in magnetic susceptibility. Based on the reported bulk susceptibility measurements [Disseler, S. M. et al., Phys. Rev. B 86, 014428 (2012)], we conclude that the sensitivity required is significantly below the typical limit of about 10^{-8} emu achievable with a high-resolution SQUID magnetometer. To address this, we have revised Figure 1b to clarify that the bounds of the CP regime are not conflated with the onset of hysteretic behavior in $R_2Ir_2O_7$.

Additionally, we thank the referee for noting that “XRMS” in Figure 1b was undefined in the text. We have corrected this labeling to “REXS” (resonant elastic X-ray scattering), which is already defined in the text. This change has also been reflected in the caption of Figure 1. We have reproduced our new Fig. 1b below (as Figure R4).

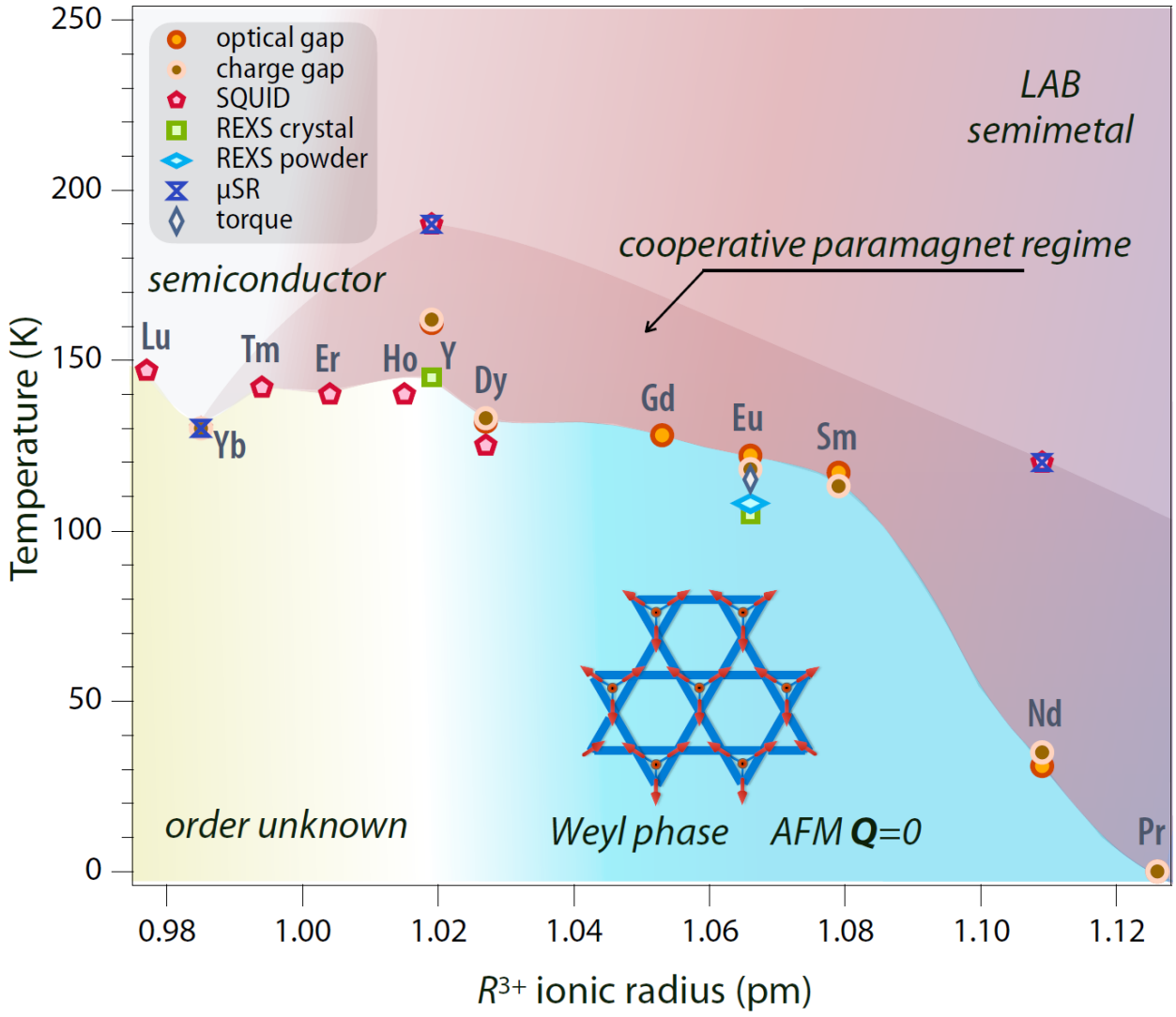

Figure R4: Modified Figure 1b of the main text.

(3) The fit of the scattering intensity versus the reduced temperature should be shown explicitly. It is not obvious that the data yields the exponent β = 0.33, indicative of the 3D Ising universality class. As different universality classes are often distinguished by only small deviations in the values of critical exponents, it is also necessary for the reader to know how stable the fit with respect to different values of β is.

We thank the referee for raising this point. The scattering intensity as a function of the reduced temperature has been fitted using the equation $I(T) = I_0 + A\left(1 - \frac{T}{T_N}\right)^{2\beta}$ where T_N = 140 K. Since the fit is primarily determined in the vicinity of the critical temperature, we tested the stability of the fitted β value by varying the range of the reduced temperature. The results indicate that β remains consistent within the range $0 < 1 - T/T_N < 0.5$, yielding a value of β = 0.30 ± 0.04.

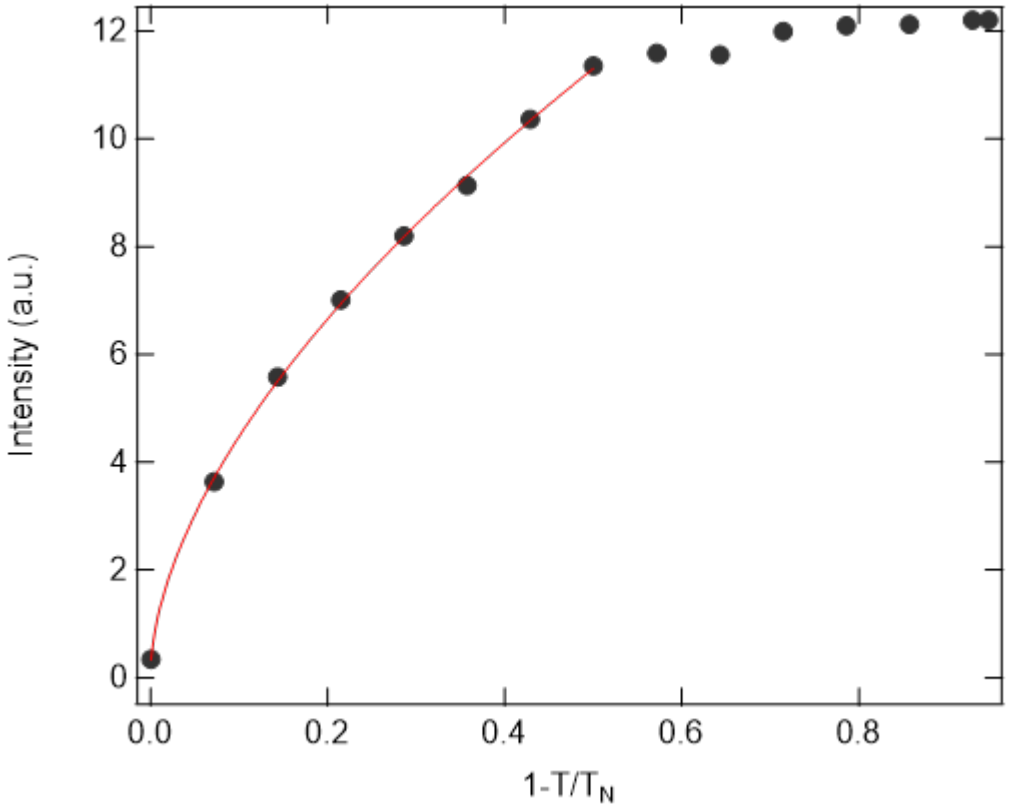

Figure R5: REXS scattering intensity as a function of $(1 - T/T_N)$.

This can be more explicitly seen by plotting the scattering intensity $I(T)$ vs. $\left(1 - \frac{T}{T_N}\right)^{0.6}$. As shown below, the linear relationship holds up to $\left(1 - \frac{T}{T_N}\right)^{0.6} < 0.66$.

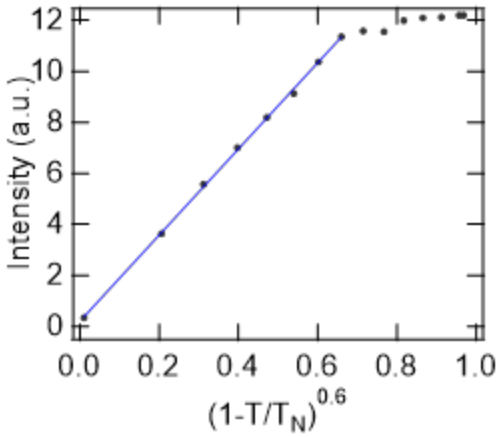

Figure R6: REXS scattering intensity as a function of $\left(1-\frac{T}{T_N}\right)^{0.6}$, corresponding to the value of β = 0.3.

To reflect this, we have added a new section to the Supplemental Material, titled "Fitting of critical exponent β", which includes Figure R6 and the following discussion:

"The REXS scattering intensity was fitted against the reduced temperature using $I(T) = I_0 + A\left(1-\frac{T}{T_N}\right)^{2\beta}$, with T_N = 140 K. As shown in Figure S4, the fitted value of β = 0.30 ± 0.04 remains robust up to $(1 - T/T_N)^{0.6} < 0.66$."

Additionally, we have updated the main text to reflect the revised value of β, including the error bars, and have referenced the Supplemental Material accordingly.

"Further, fitting the local magnetic moment M deduced from scattering intensity $I_{0\,0\,10} \propto \langle M_{Ir}\rangle^2 \propto (T_N - T)^{2\beta}$ yields a critical exponent β of 0.30 ± 0.04 (see Supplemental Material S4)."

(4) Is the magnetic continuum, which is subtracted from the inelastic scattering signal, temperature independent? From what I understand from Sec. S4 in the Supplementary Information, this seems to be the case; however, I feel this is an important information that should be mentioned explicitly in the main text.

We thank the referee for this question. Based on our analysis, the magnetic continuum exhibits negligible temperature dependence. To demonstrate this, Figure R7 presents the temperature-dependent RIXS spectra without any intensity offset, covering the range from 20 K to 175 K. As shown, the high-energy-loss region in each spectrum - dominated by the magnetic continuum - remains unaffected by temperature variations. Specifically, before subtraction, we fit the magnetic continuum in each spectrum to an anti-symmetrized Lorentzian function, as detailed in the Supplementary Information. This is also illustrated in

Figure R8, which shows an average energy of 78 meV and a full width at half maximum (FWHM) of 223 meV for the continuum.

To clarify, we have updated the following sentence in the main text:

"To further analyze this behavior, we extracted the magnetic spectral weight by removing the elastic line and the temperature-independent inelastic magnetic continuum."

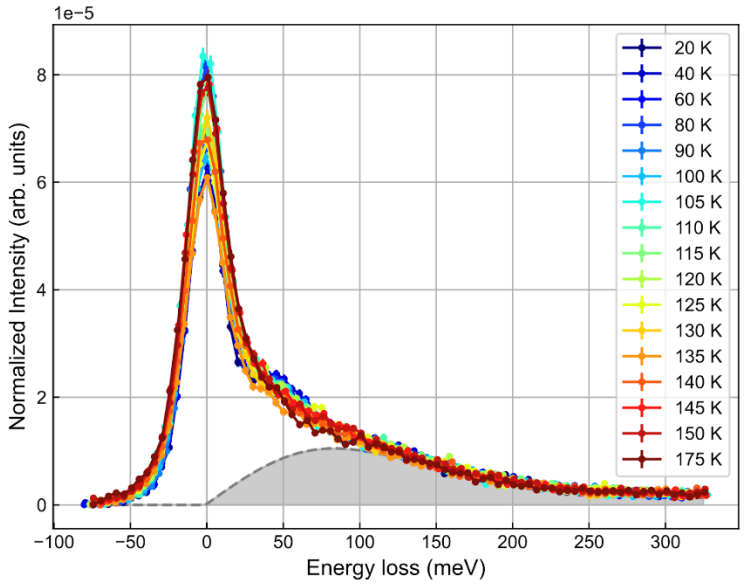

Figure R7: Temperature-dependent RIXS spectra. The temperature range of RIXS spectra is from 20 K to 175 K. The gray region is the average magnetic continuum.

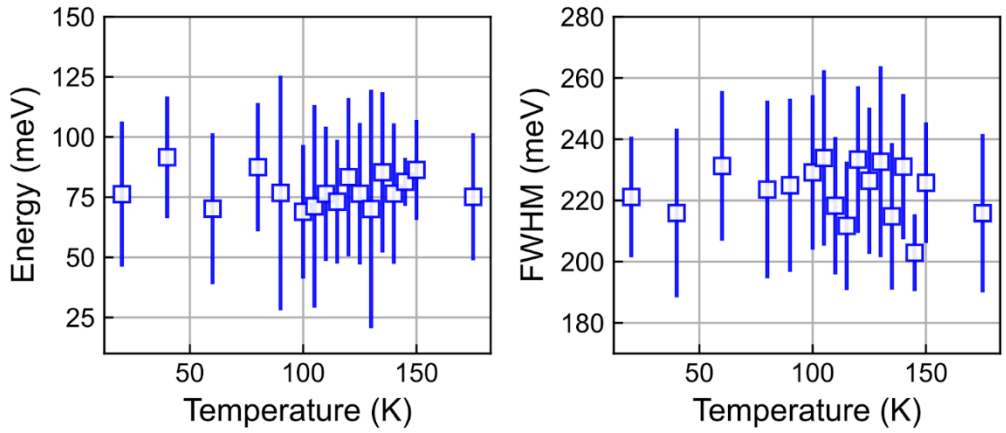

Figure R8: Temperature-dependent fitted energy and FWHM of this magnetic continuum, respectively.

(5) In the context of the interpretation of the magnetic continuum, the authors mention "the spontaneous decay of the magnon modes" as a possible origin. What kind of magnon decay do the authors have in mind? (Scattering of magnons with electronic degrees of freedom? Multi-magnon decay? Something else?)

We thank the referee for this comment. We agree that this statement could be made clearer.

Particularly, in our data the broad spectral feature extending to approximately 200 meV reflects (i) enhanced magnon-magnon scattering/decay due to strong spin fluctuations leading to the redistribution of the spectral weight across a continuum of energies, and (ii) the suppression of long-range magnetic ordering by geometric frustration which amplifies quantum fluctuations and further destroys magnon coherence.

Here we take this opportunity to connect this experimental finding to our dynamic spin susceptibility calculations (presented at the end of the Results section of the main text and Supplementary Information Section S8), which confirms the following: (1) the diffuse high energy peak is linked to the particle-hole continuum and (2) indeed is magnetic in origin. Importantly, these diffuse modes provide a spectroscopic signature of the so-called cooperative paramagnet (CP) and are not the remnants of the time-reversal symmetry-broken state.

The presence of the paramagnons persisting well above the Néel temperature indicate one of two possible scenarios: (a) that local moments remain present at high energies, or (b) that the observed spectrum is the intrinsic feature of the cooperative paramagnetic state. Sharp low-energy paramagnons and the minimal dependence of the continuum on the temperature motivated us to explore the latter scenario. Our electronic structure calculations of the DOS show two peaks - one at the Fermi energy and one in the hole-doped part of the spectrum, which already hint at the possibility for the particle-hole continuum centered at finite frequency that corresponds to this energy gap ΔE. Resolving the spin- and charge- channels of the Lindhard function (which can be done for the band structure that includes spin-orbit coupling), we find that the continuum at Γ centered at ΔE appears only in the spin susceptibility channel and is not in the charge susceptibility channel. This implies the fully magnetic nature of the continuum ascribed to Stoner excitations.

To clarify these findings, we have modified the sentence in the main text as follows:

"The origin of the continuum was previously proposed as arising from the spontaneous multi-magnon decay [Zhitomirsky, M. E. & Chernyshev, Rev. Mod. Phys. 85, 219–242 (2013)] or, more broadly, incoherent multi-magnon excitations [Chun, S. H. et al., Phys. Rev. Lett. 120, 177203 (2018)]. In particular, we attribute the origin of this peak to the particle-hole continuum. Decomposing the calculated Lindhard function into its spin and charge channels shows that the continuum appears exclusively in the spin susceptibility channel and absent in the charge channel."

(6) It is interesting that the observed sharp magnon dispersion is very flat; namely, the band width appears to be significantly smaller than the gap, and the two bands appear to be well separated. This is a remarkable feature, which is also not well reproduced by the spin-wave calculation and the ab-initio dynamical susceptibility calculations. Do the authors understand the origin of this phenomenon?

We thank the referee for the insightful comment. Theoretically, for our system four branches of magnetic excitations are expected. However, given the current RIXS resolution of 28 meV and the close spacing in energy of at least two of the four branches at the same momentum q, it is experimentally feasible to resolve only 2-3 branches under most optimal conditions. Furthermore, based on the calculated S(q,ω), certain branches contribute minimally to the RIXS spectra due to their very small spectral weight. The lower branch we observed corresponds to the lowest-lying branches, which are relatively flat in the theoretical calculations. For example, in $Sm_2Ir_2O_7$, the lowest branch has a bandwidth of ~2 meV in the calculation. However, this branch was not experimentally resolved, likely due to its weak spectral weight.

The upper magnon branch in our work is indeed flatter than that in other $R_2Ir_2O_7$. To illustrate this point, as a comparison, Figure R9 reproduces Figure 4 from Ref. 46 [Donnerer, C. et al. Phys. Rev. Lett. 117, 037201 (2016)]. As seen, when comparing $Sm_2Ir_2O_7$ (Ref. 46) with $Y_2Ir_2O_7$ (this work), we note that the highest magnon energy in $Y_2Ir_2O_7$ is slightly higher, reaching 50 meV compared to 45 meV in $Sm_2Ir_2O_7$. On the other hand, the magnon gap at Γ in $Y_2Ir_2O_7$ is 42 meV, which is significantly larger than the ~25 meV gap observed in $Sm_2Ir_2O_7$.

As correctly pointed by the referee this bandwidth is not well-produced in the linear spin-wave calculations which currently only includes the Heisenberg J and the DM interactions. We suspect that additional, longer-range terms such as ring exchange are necessary. A similar conclusion was reached for the square-lattice antiferromagnet La_2CuO_4, where a ring-exchange term was required to match the experimental results [Coldea *et al.*, Phys. Rev. Lett. 86, 5377 (2001)]. It is plausible that a comparable effect is at play in our system. When viewed along the [111] crystallographic direction (the film normal), the pyrochlore structure can be decomposed into alternating two-dimensional triangular and kagome planes, which is a geometry in which ring exchange arises naturally.

We note that in the phase diagram of Fig. 1, both Sm and Eu are far away from Y. As the result, the magnon dispersion observed below the Néel temperature in $Y_2Ir_2O_7$ cannot simply be inferred from these other systems. Nevertheless, due to the severe geometrical constraints from the thin-film nature of our sample, we are currently unable to determine the complete magnon dispersion along all high-symmetry directions. With further advances in synthesis of bulk $Y_2Ir_2O_7$ it should be possible to more reliably extract magnetic interactions, including the proposed ring exchanges, by examining magnon dispersions over larger regions of reciprocal space.

The curious atypical observation of flat magnon bands, as pointed by the referee, indeed motivated us to explore CP regime above T_N in $Y_2Ir_2O_7$ via the ab-initio + dynamical susceptibility calculations. At the level of the Lindhard function alone, we were unable to reproduce the experimentally observed flat bands. However, a more thorough treatment of the short-range interactions that are expected to be present in the material, e.g. within the random phase approximation (RPA) approach [e.g. Lee et al., Phys. Rev. B 87, 214416 (2013)], are expected to show the renormalization of some features in the spectra, as was seen in other correlated electron systems, see e.g. Refs. 99-101. $Y_2Ir_2O_7$ indeed presents itself as a great candidate for a full theoretical RPA study.

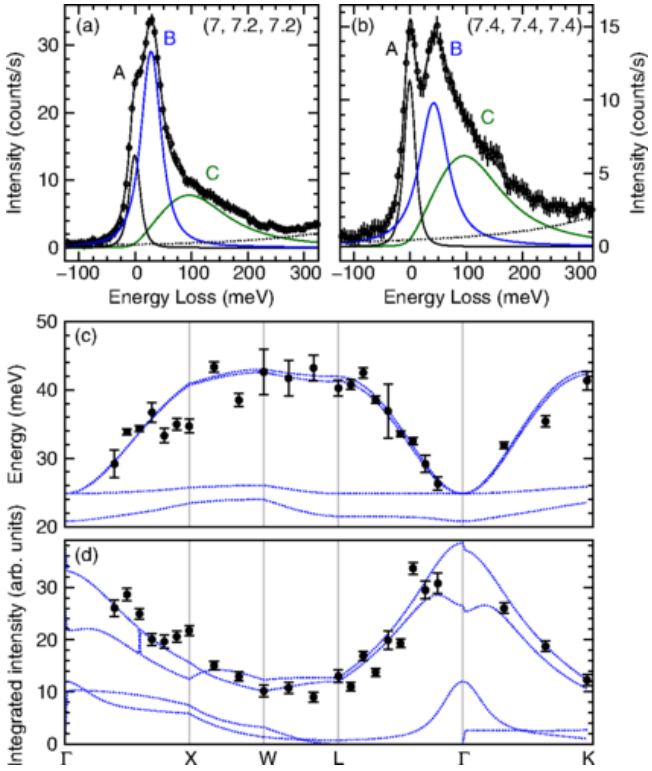

Figure R9: (Top) RIXS spectra away from zone center along (0 L L) and (L L L) directions. (Bottom) Spin-wave fits to experimental data. Reproduced from [46].

We have added the following discussion:

"We note that the linear spin-wave fit does not fully capture the behavior of the higher-energy mode near Γ. One possibility is that higher-order interactions (e.g., ring exchange) may be necessary to fully capture the spin-wave behavior [Coldea et al., Phys. Rev. Lett. 86, 5377 (2001)]. The improvement in the synthesis of high-quality bulk single crystals may allow for the study of dispersion along more high-symmetry directions, clarifying the role of higher-order corrections in the spin-wave dynamics in $Y_2Ir_2O_7$. Alternatively,

calculating the dynamical structure factor within the random-phase approximation (RPA) may be more appropriate for some pyrochlore iridate compounds [Lee et al., Phys. Rev. B 87, 214416 (2013)]; recent work on non-stoichiometric $Tb_2Ir_2O_7$ also signals that the RPA approach may better fit the dispersion of the smaller rare-earth site pyrochlore iridate compounds [Faure, Q. et al. ArXiv:2404.03829 (2024)]."

(7) In the spin-wave analysis, a model with Heisenberg, Dzyaloshinskii–Moriya, and symmetric off-diagonal Gamma interaction is used. Symmetry would allow, however, a Kitaev-type bond-dependent interaction, see, e.g., [Phys. Rev. X 1, 021002 (2011); Phys. Rev. B 95, 094422 (2017)]. It is not obvious to me why this exchange interaction can be neglected. To the contrary, it would be interesting to know whether taking this interaction into account can improve the agreement between experiment and spin-wave analysis.

We thank the referee for this insightful question. The referee is correct that symmetry permits four independent nearest-neighbor interactions. The Kitaev-type interaction (perhaps in context better thought of as an Ising anisotropy with respect to local axes), is already partially accommodated for by the Γ interaction. We note that the Γ interaction is traceless but generally has diagonal components. We thank the referee for calling our attention to our mistake in referring to it as the "symmetric off-diagonal term" at one place in the Supplementary Information, section S7. This has been corrected in the revised manuscript.

Symmetry generically allows for one coefficient Γ_1 multiplying the diagonal components and another coefficient Γ_2 multiplying the off-diagonal components of the Γ_{ij} tensor; see, e.g., [Eq. (3) in Nat. Phys., 6, 376 (2010)]. However, strong-coupling derivations of the spin Hamiltonian in pyrochlore iridates starting from Slater-Koster constructions of the direct Ir->Ir and indirect Ir->O->Ir time-reversal-symmetric hopping processes find a fixed relationship $\Gamma_2 = 3\Gamma_1$ [see Nat. Phys., 6, 376 (2010); Phys. Rev. B 85, 045124 (2012)]. This motivates using a three-parameter model (but indeed not one where the Γ interaction is purely off-diagonal).

Nevertheless, as argued in [Phys. Rev. Research 2, 043273 (2020)] this fixed relationship between the diagonal and off-diagonal coefficients can break down in more general models. We have attempted fitting the data also using the general four-parameter model (J, D, Γ_1, Γ_2) but have not been able to obtain robust results. We attribute this to optimization challenges arising from two main issues: (i) when the two Γ coefficients are allowed to vary independently they can rapidly modify the magnetic order and (ii) the model is overparameterized, i.e., the number of fitted parameters is too large for the limited number of data points, leading to a flat fitness landscape. For these reasons we chose to not report any fits for the four-parameter model, but we agree that it would be worthwhile to revisit this decision when future experiments collect more data over a wider area of reciprocal space. We have updated Section S7 of the Supplementary Information to include these considerations and cite [Phys. Rev. Research 2, 043273 (2020)].

We have revised Section S7 as follows:

"The traceless symmetric anisotropic term was neglected in the main text, but is included here for completeness."

We also added the following:

"In principle, symmetry also allows for the nearest-neighbor symmetric anisotropic exchange to be parameterized by two independent parameters Γ_1 and Γ_2 [16]. These are found to be proportional to each other in perturbation-theory derivations of the spin Hamiltonian [12,13], motivating the use of two- and three-parameter models here, but we note that this relationship can break down in more general models [16]. We have attempted to fit our data also to the four-parameter model (J,D,Γ_1,Γ_2) but did not obtain robust fitting results, presumably due in part to the limited amount of data.

We have performed classical Monte Carlo simulations using the ESpinS software [17] to estimate the ordering temperature of the two-parameter model. We find a T_N of at least 127 K in reasonable agreement with the experimental value; see Figure S8. The T_N value extracted from specific heat grows with system size and could further approach the experimental value of 145 K in the thermodynamic limit. Due to uncertainties with fitting and simulation, as well as the expectation that quantum effects could renormalize the value, we have not carried out a detailed finite-size scaling here. The simulations used clusters with N=4 x L x L x L sites. Following Ref. [14] 10^6 Monte Carlo steps were used for thermalization, and 2 * 10^6 steps were used for the sampling."

Finally, we added the following sentence to the linear spin wave modeling section of Methods:

"We have also performed a classical Monte Carlo simulation for the fitted model that supports an AFM transition at $T_N \geq \sim$127 K, a value reasonably close to the experimental critical temperature of 145 K. See Sec. S7 in the Supplementary Information for details."

(8) What is the evidence for the statement that "the ratio between the competing interactions, D/J ~ 0.17, is in line with the experimental value of T_N = 145 K"? What is the theoretical value of T_N in the model with J = 33.9meV and D = 5.6 meV?

We thank the referee for raising this question. The purpose of the original statement was to indicate that the energy scales are in the correct range. To further clarify this, we have carried out a classical Monte Carlo simulation using the ESpinS package [N. Rezaei et al., Comput. Mater. Sci. 202, 110947 (2022); https://github.com/nafiserb/ESpinS] on clusters of up to $N = 4 * 20^3$ sites for the model in question, finding a T_N of at least 127 K; see the Figure R10. Panel (a) shows magnetic specific heat and (b) shows the temperature dependence of the 4i-4o order parameter.

The T_N value extracted from specific heat grows with system size and could further approach the experimental value of 145 K (indicated by vertical dashed line) as one approaches the thermodynamic limit. Due to uncertainties in the fitting procedures and simulations, as well as the anticipated renormalization by quantum effects, we have not conducted a detailed finite-size scaling analysis in this work.

In addition, one can also obtain an approximate result by comparing with the Monte Carlo results shown in Figure 4(top) in [M. Elhajal et al., Phys. Rev. B 71, 094420 (2005)] where the authors reported a transition around T/J~0.28 for D/J=0.1. Since the $D = 0$ model does not order classically, the transition temperature should be proportional to D. It appears Elhajal et al. used the convention that $|D = D_{ij}|$, which we can correct for by scaling it by $\sqrt{2}$. By this approach we obtain $T_N = 0.17/(0.1 * \sqrt{2}) * 0.28 * (33.9\ meV) = 132\ K$, in reasonable agreement with the results from our own Monte Carlo simulations.

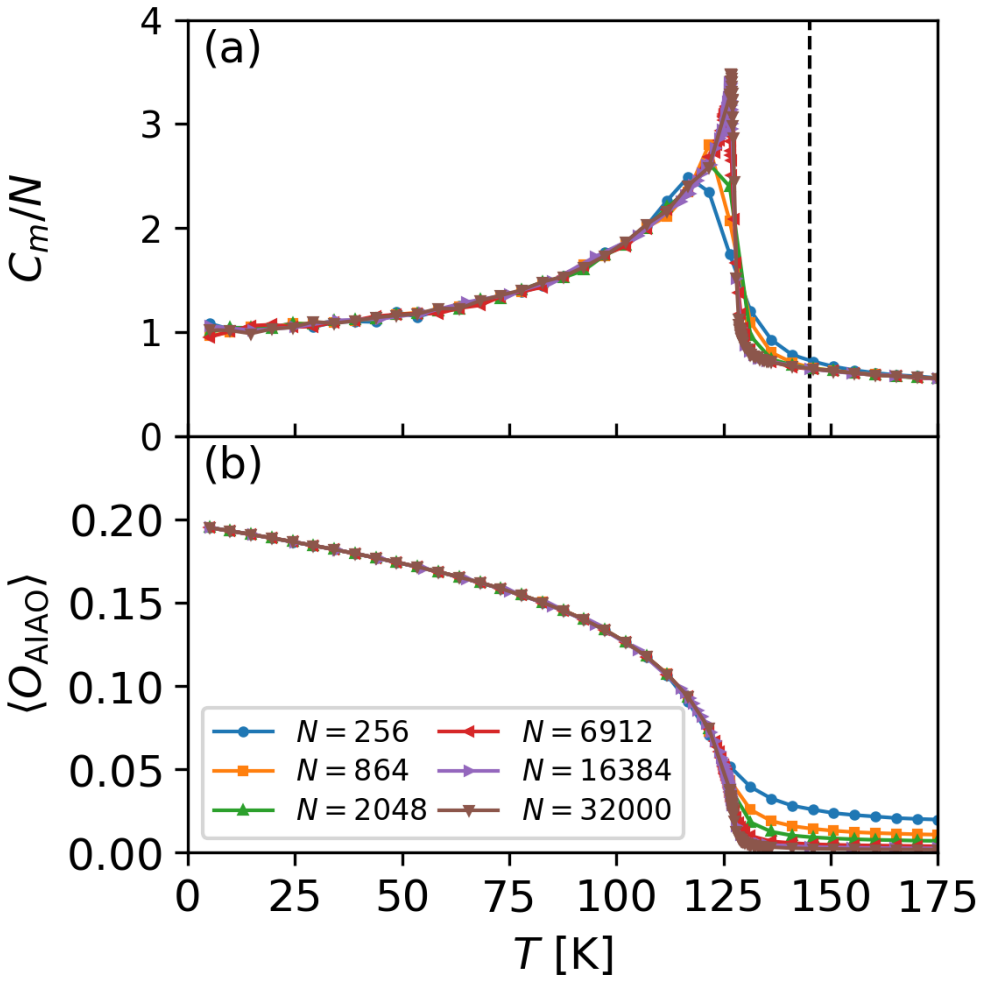

Figure R10: Classical Monte Carlo simulations. (a) Magnetic specific heat predicts a transition temperature of at least $T_N \approx 127$ K. The dashed vertical line indicates the experimentally observed transition temperature 145 K. \textbf{b} the four-in-four-out order parameter. All calculations were done for the best fitted two-parameter model with $J = 33.9$ meV and D =5.6 meV on clusters with $N = 4L^3$ sites.

(9) Fig. 4b: The figure shows a metallic density of states, but the caption mentions "the paramagnetic state [...] above the topologically-trivial insulator phase". This should be explained.

We thank the referee for this comment. A ground state, the magnetically ordered 4i-4o *insulating* state, does indeed exhibit a gapped density of states (not included in the manuscript). The DOS presented in Figure 4b of the main text corresponds to the paramagnetic phase ($T > T_N$), above the insulating 4i-4o ground state. Numerically, it is not uncommon, nor is it a violation of any principles, for the DOS in paramagnetic phase to appear *metallic*, as is the case here.

The so-called paramagnetic (PM) state at $T > T_N$ is obtained using DFT+U calculations in a mean-field approximation. We initialized the magnetic configuration at each site to be exactly zero, with noncollinear magnetic self-consistent field calculations converging to a zero-magnetic-moment final state without on-site spin fluctuations. Simulating a true paramagnetic state would require random sampling of spin configurations within large supercells, which is beyond the scope of our current calculations.

(9) Fig. 4c: What is the integration volume around the Brillouin zone center used in this plot? It is confusing that Fig. S6c in the Supplementary Information indicates that the gap of the magnetic excitations at the Brillouin zone center is smaller than a few meV, and possibly zero, while Fig. 4c and the main text, mentioning a "low-energy peak centered around 25 meV", implicitly suggest a finite gap. This should be explained.

The integration around the zone center in Figure 4c is obtained by summing over 3×3×3 q-points, considering linear sizes of 5% around Γ. For volumes up to 10% of the Brillouin zone around Γ the position of the peak moves just slightly away from 25 meV; with the width of the peak increasing with the volume considered. While our calculations capture other features of the spectrum well, they do not reproduce the gap observed experimentally.

The inconsistency between the gap in the experiment and the calculations remains to be resolved, one possibility being a very sharp DOS at $E = E_F$ with the Fermi surface showing pronounced nesting from the cube-like pocket at $q \sim 0$. The way to resolve this would be to better account for the electronic correlations, e.g., within the RPA approximation which is known to renormalize the effects of the spurious gapless excitations originating from the Fermi surface nesting by attributing it much less weight in the imaginary part of the susceptibility. The RPA approach to this problem goes beyond the scope of this work.

To clarify this, we have added the following line to the discussion of the susceptibility calculations:

"While our calculations (on the level of Lindhard function calculation) very well capture the high-energy excitations, and the presence of two magnon branches in the low-energy excitations (as discussed in the Supplementary Information), they do not reproduce the experimentally observed gap magnitude."

Additionally, we clarified the following sentence:

"As seen, all models qualitatively exhibit the same response, featuring a low-energy peak centered around 25 meV and a higher-energy broader peak centered at approximately 70-90 meV. We note, however, that the position of the low-energy peak does not correspond to the gap of the lowest excitations, which appear to be gapless in our calculations, as is discussed in the Supplementary Information. The inconsistency between the gap in the experiment and the calculations remains to be resolved, likely within a more advanced model that better accounts for electronic correlations in the system."

(10) The statement that "the signs of the zero-temperature transition from the PyIr Weyl semimetal to the paramagnetic metallic phase are attributed to [...] the emergence of gapless fermions due to the breaking of an emergent internal SO(3) symmetry (Ref. 27)" is confusing. First, at the quantum critical point discussed in Ref. 27, additional gapless fermions are not expected to emerge, since both sides of the transition are semimetallic. Second, it is not clear what is meant with breaking of an emergent symmetry. In my understanding, a symmetry cannot be both emergent and broken at a single point in parameter space.

We thank the referee for this comment. We agree that this statement detracts from the main point of the paragraph. Accordingly, we have removed the following sentences from the text:

"Specifically, the signs of the zero-temperature transition from the PyIr Weyl semimetal to the paramagnetic metallic phase are attributed to the cube-like shape of the Fermi surface and the emergence of gapless fermions due to the breaking of an emergent internal SO(3) symmetry. Both features are evident in our first-principles calculations based on a realistic model of a $Y_2Ir_2O_7$ finite slab."

In conclusion, the paper presents significant experimental results that could be of great interest to a broad audience. However, the current version lacks clarity in the interpretation of the data. I recommend inviting the authors to submit a substantial revision of the manuscript.

We revised the manuscript addressing all referee comments, and we hope the current form is satisfactory to the referee.

Complete list of revisions to manuscript

Main text:

"...we unequivocally reveal the presence of spectrally sharp, gapped magnetic excitations in $Y_2Ir_2O_7$ that surprisingly persist well above the Néel transition temperature, signaling the presence of a universal regime connected to fluctuations on frustrated lattices."

"The rare-earth element has a significant impact on the structural and electronic properties of the pyrochlore iridates. Like the other compounds on the left-hand side of the diagram, Y2Ir2O7 exhibits semiconducting behavior (see Supplementary Information Fig. S2), sharply contrasting with the metallic behavior for R=Eu and beyond."

Modified Figure 1b

"Further, fitting the local magnetic moment M deduced from scattering intensity $I_{0\,0\,10} \propto \langle M_{Ir} \rangle^2 \propto (T_N - T)^{2\beta}$ yields a critical exponent β of 0.30 ± 0.04 (see Supplemental Material S3)."

"We note that this value differs from the critical exponent β=0.2 as found in Eu2Ir2O7) [Chun, S. H. et al., Phys. Rev. Lett. 120, 177203 (2018)]. This finding, in conjunction with the difference in resistivity behavior near T_N, implies that the magnetic behavior in Y2Ir2O7 may be markedly different compared to Eu2Ir2O7."

"The origin of the continuum was previously proposed as arising from the spontaneous multi-magnon decay [Zhitomirsky, M. E. & Chernyshev, Rev. Mod. Phys. 85, 219–242 (2013)] or, more broadly, incoherent multi-magnon excitations [Chun, S. H. et al., Phys. Rev. Lett. 120, 177203 (2018)]. In particular, we attribute the origin of this peak to the particle-hole continuum. Decomposing the calculated Lindhard function into its spin and charge channels shows that the continuum appears exclusively in the spin susceptibility channel and absent in the charge channel."

"A direct comparison of the experimental dispersion curves to the linear spin-wave theory gives the values of the magnetic interactions $J = 33.9$ meV and $D = 5.6$ meV (see the Supplementary section S5); these values are in line with the Raman spectroscopy work on Y2Ir2O7 [Nguyen, T. et al. Phys. Rev. Lett. 127, 267203 (2021)]."

"We note that the linear spin-wave fit does not fully capture the behavior of the higher-energy mode near Γ. One possibility is that higher-order interactions (e.g., ring exchange) may be necessary to fully capture the spin-wave behavior [Coldea et al., Phys. Rev. Lett. 86, 5377 (2001)]. The improvement in the synthesis of high-quality bulk single crystals may allow for the study of dispersion along more high-symmetry directions, clarifying the role of higher-order corrections in the spin-wave dynamics in $Y_2Ir_2O_7$. Alternatively, calculating the

dynamical structure factor within the random-phase approximation (RPA) may be more appropriate for some pyrochlore iridate compounds [Lee et al., Phys. Rev. B 87, 214416 (2013)]; recent work on non-stoichiometric $Tb_2Ir_2O_7$ also signals that the RPA approach may better fit the dispersion of the smaller rare-earth site pyrochlore iridate compounds [Faure, Q. et al. ArXiv:2404.03829 (2024)]."

"To further analyze this remarkable behavior, we extracted the magnetic spectral weight by removing the elastic line and the temperature-independent inelastic magnetic continuum."

"The persistence of the unusual magnetic gap, even as the long-range magnetic order melts, is unexpected and unique, standing in sharp contrast to the previous RIXS reports on pyrochlore iridates. $Sm_2Ir_2O_7$ shows the spectral weight for the magnon mode disappear around the transition temperature [Donnerer, C. et al., Phys. Rev. Lett. 117, 037201 (2016)], whereas Eu2Ir2O7 shows the gap softening at Γ as T approaches T_N [Chun, S. H. et al., Phys. Rev. Lett. 120, 177203 (2018)]. Y2Ir2O7 is perhaps a more likely candidate for observing the persistent gapped magnetic excitations since the system lacks a confounding structural phase transition or the renormalization of the Heisenberg interaction observed in Eu2Ir2O7. We speculate that this could result from Ir-O-Ir bond angle and Ir-O bond length differences across the pyrochlore iridate family, leading to a deviation of the $J_{1/2}$ significantly away from the idealized equal superposition of Ir d_{xy}, d_{yx} and d_{zx} orbitals [G. Jackeli and G. Khaliullin, Phys. Rev. Lett. 102, 017205 (2009)]."

"As seen, all models qualitatively exhibit the same response, featuring a low-energy peak centered around 25 meV and a higher-energy broader peak centered at approximately 70-90 meV. We note, however, that the position of the low-energy peak does not correspond to the gap of the lowest excitations, which appear to be gapless in our calculations, as is discussed in the Supplementary Information. The inconsistency between the gap in the experiment and the calculations remains to be resolved, likely within a more advanced model that better accounts for electronic correlations in the system."

"While our calculations (on the level of Lindhard function calculation) very well capture the high-energy excitations, and the presence of two magnon branches in the low-energy excitations (as discussed in the Supplementary Information), they do not reproduce the experimentally observed gap magnitude."

Removed: "Specifically, the signs of the zero-temperature transition from the PyIr Weyl semimetal to the paramagnetic metallic phase are attributed to the cube-like shape of the Fermi surface and the emergence of gapless fermions due to the breaking of an emergent internal SO(3) symmetry. Both features are evident in our first-principles calculations based on a realistic model of a Y2Ir2O7 finite slab."

"We have also performed a classical Monte Carlo simulation for the fitted model that supports an AFM transition at $T_N \geq \sim 127$ K, a value reasonably close to the experimental critical temperature of 145 K. See Sec. S7 in the Supplementary Information for details."

"We have identified the range $U \leq 0.9$ eV as the region where the ground state exhibits a Weyl semimetal phase (with small electron and hole pockets near $U = 0.9$ eV), beyond which the system transitions to an insulating state. See Supplementary Information, Section S9, for additional details. As seen, the 4-in/4-out magnetic ordering remains robust for all values of $U \geq 0.75$ eV. Using linear response theory within the DFT+U framework [Cococcioni, M. & de Gironcoli, S. Phys. Rev. B 71, 035105 (2005).] we estimated the effective U for Ir d-orbitals to be 1.96 eV, at which the ground state of $Y_2Ir_2O_7$ appears as a 4-in/4-out insulator with a small gap of 0.38 eV."

"We used the rotationally invariant approach for DFT+U [Dudarev et al., PRB 57, 1505 (1998)], with a single Hubbard U parameter correlating the d-shell of the Ir sites. Comparisons of the electronic structures obtained from DFT+eDMFT are provided in the Supplementary Material sections S12 and S13."

Supplemental information:

Section S2: Added Figure R2 and caption. Added: "To compare the resistivity behavior between $Y_2Ir_2O_7$ and $Eu_2Ir_2O_7$, electrical transport measurements were taken between 2K and 300K. Measurements were taken at Rutgers University with a Physical Properties Measurement System manufactured by Quantum Design. Fig. S2 shows that $Eu_2Ir_2O_7$ has a minimum in resistivity around 105 K, indicating a metal-insulator transition at T_N. $Y_2Ir_2O_7$ lacks such a transition, instead resembling more semimetallic behavior."

Section S4: Added Figure R6 and caption. Added: "The REXS scattering intensity was fitted against the reduced temperature using $I(T) = I_0 + A\left(1 - \frac{T}{T_N}\right)^{2\beta}$, with T_N = 140 K. As shown in Figure S4, the fitted value of $\beta = 0.30 \pm 0.04$ remains robust up to $(1 - T/T_N)^{0.6} < 0.66$."

Section S7: "The traceless symmetric anisotropic term was neglected in the main text, but is included here for completeness."

Added: "In principle, symmetry also allows for the nearest-neighbor symmetric anisotropic exchange to be parameterized by two independent parameters Γ_1 and Γ_2 [16]. These are found to be proportional to each other in perturbation-theory derivations of the spin Hamiltonian [12,13], motivating the use of two- and three-parameter models here, but we note that this relationship can break down in more general models [16]. We have attempted to fit our data also to the four-parameter model (J,D,Γ_1,Γ_2) but did not obtain robust fitting results, presumably due in part to the limited amount of data.

We have performed classical Monte Carlo simulations using the ESpinS software [17] to estimate the ordering temperature of the two-parameter model. We find a T_N of at least 127 K in reasonable agreement with the experimental value; see Figure S8. The T_N value extracted from specific heat grows with system size and could further approach the experimental value of 145 K in the thermodynamic limit. Due to uncertainties with fitting and simulation, as well as the expectation that quantum effects could renormalize the value, we have not carried out a detailed finite-size scaling here. The simulations used clusters with N=4 x L x L x L sites. Following Ref. [14] 10^6 Monte Carlo steps were used for thermalization, and 2 * 10^6 steps were used for the sampling."

Added Fig. R10 and caption

Section S13: "In this section, we present the results of the electronic structure calculations obtained using DFT+embedded dynamical mean-field theory (eDMFT) for the paramagnetic phase of Y2Ir2O7. The DFT part of the calculation is performed using the WIEN2K code [38], using an all-electron LAPW basis set and a PBE exchange-correlation functional on a Monkhorst-Pack mesh of 11x11x11 k points. We have thoroughly checked that the electronic structures obtained by the VASP and WIEN2K agree when U=0. The eDMFT calculations [39-41] start with projecting to a set of real-space orbitals that span the correlated subspace, and the bath orbitals are treated by DFT. The hybridization between the impurity and the bath is then self-consistently determined by solving the DMFT equations. The projector is chosen to be the atomic-like t2g orbitals of one isolated Ir atom. A window of 20 eV around the Fermi level is used for computing the hybridization between the impurity and the bath, and during the self-consistency loops, continuous time quantum Monte Carlo [42, 43] was performed to solve the quantum impurity until the charge density, the impurity self-energy, and the lattice Green's function are converged. The double-counting correction is computed using the nominal double-counting scheme [39, 43]. Then the maximum entropy method [44] is used to perform the analytical continuation of the self-energy to real frequencies.

Figure S11 shows a comparison between the electronic structures of bulk Y2Ir2O7 computed using DFT+eDMFT (a-b, paramagnetic state) and DFT+U (c-d, zero local spin magnetic moments are assumed).
We notice that eDMFT captures the metal-insulator transition of the system around U=5.0 eV. In contrast, when using DFT+U, the system remains metallic even with a large U. This is because in our DFT+U calculations, we have constrained the local spin magnetic moments to be zero. The on-site spin fluctuations would only be accessible if the disordered local moments approach [45] is used. We highlight the similar two-peak feature in the DOS that appears at the Fermi level in the metallic regime from both DFT+U and DMFT results,

suggesting that one would expect to see a similar behavior in their transverse spin susceptibilities."

Added Fig. R3 and caption

Additional changes to main text:

Added Ref: Jackeli, G. & Khaliullin, G. Phys. Rev. Lett. 102, 017205 (2009).

Added Ref: Dudarev, S. L. et al. Phys. Rev. B 57, 1505–1509 (1998).

Added Ref: Faure, Q. et al. ArXiv:2404.03829 (2024).

Added acknowledgements to Yihua Qiang and Kristjan Haule

Added Data Availability and Code Availability statements